Comparing sparse inertial sensor setups for sagittal-plane walking and running reconstructions

Eva Dorschky[1◕] Marlies Nitschke[1◕] Matthias Mayer[1] Ive Weygers[2] Heiko Gassner[3,4] Thomas Seel [5] Bjoern M. Eskofier[1] Anne D. Koelewijn[1*]

◕These authors contributed equally to this work and share first authorship
1 Machine Learning and Data Analytics Lab, Department Artificial Intelligence in Biomedical Engineering (AIBE), Friedrich-Alexander-Universität Erlangen-Nürnberg (FAU), Erlangen, Germany
2 Intelligent Sensorimotor Systems Lab, Department Artificial Intelligence in Biomedical Engineering (AIBE), Friedrich-Alexander-Universität Erlangen-Nürnberg (FAU), Erlangen, Germany
3 Department of Molecular Neurology, University Hospital Erlangen, Erlangen, Germany
4 Digital Health Systems, Fraunhofer Institute for Integrated Circuits IIS, Erlangen, Germany
5 Institute of Mechatronic Systems, Leibniz Universität Hannover, Hannover, Germany
¤Carl-Thiersch-Str. 2b, 91052 Erlangen, Germany
* anne.koelewijn@fau.de

Abstract

A sensor setup with a small number of sensors, i.e., a sparse sensor setup, could enable a comprehensive unobtrusive motion analysis using inertial motion capture (IMC) with little obtrusion to the user, which is critical for clinical and sports applications, such as assessing disease, providing biofeedback in rehabilitation, or enhancing performance in sports. When sparse sensor setups were used, the motion analysis was either not comprehensive or physical correctness was not considered. Furthermore, the relationship between sensor setup and the resulting accuracy of spatiotemporal, kinematic, or kinetic variables has not been investigated systematically. Therefore, we investigated the accuracy of biomechanical gait reconstructions from different sparse inertial sensor setups, in which the number of sensors is reduced by not placing sensors on all body segments of interest. We created biomechanical reconstructions by solving optimal control problems with a sagittal plane musculoskeletal model. The resulting simulations tracked raw accelerometer and gyroscope data while minimizing muscular effort. We applied this approach to six different sparse sensor setups to investigate the reconstruction quality of spatiotemporal, kinematic, and kinetic variables for each of these setups at three walking and three running speeds. We found that correlations between IMC and optical motion capture (OMC) were large for all sensor setups, but that those setups without a pelvis sensor led to a forward trunk lean that was too high, as well as unrealistic kinetics and kinematics. Spatiotemporal variable estimations generally also benefitted from a pelvis sensor, but not as much as the kinetic and kinematic estimations. We found that for setups including a pelvis sensor, there was no clear benefit for including additional sensors. While walking speed, step length, and joint kinematics generally benefited from using more sensors, the hip moment and knee moment did not. During running, the ankle moment and vertical ground reaction force were even estimated more accurately with smaller sensor setups. Therefore, we conclude

that sagittal-plane reconstruction of walking and running kinetics and kinematics using sparse sensor setups can improve usability at the cost of only minor reductions in accuracy. When using a sparse sensor setup for gait reconstructions using optimal control, we advise to always include a pelvis sensor to achieve accurate results.

Author summary

We aim to analyse walking and running in an environment that is as normal as possible. To do so, we should use sensor setups that can be worn in any environment, and that are the least bothersome to the wearer, and that ensure their privacy. Inertial sensors are small sensors that measure accelerations and velocities during movements that can be used in any environment, while also they do not record privacy-sensitive information as video cameras would. To also ensure that they are the least bothersome, while still being accurate, we investigated the accuracy of walking and running variables of different sparse sensor setups, i.e., sensor setups that do not have sensors on each body part of interest. We compared these setups to a full sensor setup, with sensors on all body parts of interest. All sensor setups included sensors measuring the feet, because those can be attached to the shoes instead of on the body, as would be required for sensors measuring the thighs or shanks. We show that movement analyses can be as accurate as with the full sensor setup using only three sensors, two on the feet and one on the pelvis. We also found that any sensor setup with no pelvis sensor led to inaccurate analysis of the trunk.

Introduction

Gait analysis is a fundamental tool for understanding human locomotion. It can provide insight into movement disorders (e.g., [1]), evaluate the quality of assistive devices such as prostheses and orthoses (e.g., [2]), or be used as a tool to improve performance and prevent injury in sports (e.g., [3]). OMC combined with force plates is currently considered the gold-standard for gait measurements required to perform gait analysis [4]. While OMC is widely-used in different application domains and leads to accurate measurements and analyses, its application is still restricted due to the necessary laboratory environment and the need for expensive equipment, such as infrared cameras and force plates [5]. Therefore, its use is currently limited to research applications and for specific diseases affecting gait, such as amputations, stroke, or cerebral palsy.

Instead, a measurement method that is cost-effective and allows for recordings "in the wild", or outside the laboratory environment, could enable widespread use of gait analysis in different clinical and sports applications. Such methods could for example be markerless motion capture, based on video images, or IMC. First, video-based motion capture [6, 7] still requires the person to be in the camera's field of view. Moreover, lighting conditions, camera placement, and occlusion can affect the accuracy, limiting the flexibility of the system. Second, IMC systems record motion using a setup of inertial measurement units (IMUs), which are small, low cost, wearable sensors that contain an accelerometer and a gyroscope, and sometimes a magnetometer [8]. These sensors are attached to different body segments to measure their linear accelerations and angular velocities, as well as possible other signals. Since this approach is based on wearable sensors, IMC can be used to measure movement in natural conditions in any environment [9].

While many different methods have been developed to estimate spatiotemporal variables (see [10] for a review) and kinematics (see [5] for a review) of movements from inertial sensor data, estimation of kinetics is more challenging. However, kinetic

information is required to understand the mechanical and physiological mechanisms of human movement. One approach that has been proposed is to estimate ground reaction forces from inertial sensor data (see [11] for a review of these approaches), which can then be combined with the kinematic data to perform a traditional inverse dynamics analysis [12]. This approach can also be extended with static or dynamic optimization to determine muscle forces and activations as well, but then several calculation steps are required to obtain all kinetic and kinematic information. Furthermore, this approach requires a double integration of the measured acceleration signals to obtain kinematics, meaning that the resulting kinematics will likely be affected by integration drift [13]. Another approach to process IMC data is to train a machine learning model to estimate joint kinetics and kinematics (e.g. [14–18]), but these models are either based on virtual data [14], only estimate kinematics [15, 16], or require a full sensor setup [18]. Furthermore, machine learning models are typically trained and tested using lab-based OMC and IMC data, which means that there is no proof that such a model will perform well "in the wild" as interpretation of the model output is challenging. Another major challenge when applying machine learning to estimate joint kinetics and kinematics is the availability of training data since the machine learning model accuracy has been shown to improve with the size of the training dataset [19].

We have developed an optimal control approach to estimate kinetics and kinematics of walking and running based on measurements from only accelerometers and gyroscopes, which inherently overcomes the aforementioned drift problems [20]. In this approach, an optimal control problem is solved to find a simulation for a sagittal plane musculoskeletal model that minimizes effort while also minimizing a tracking error between virtual and measured inertial sensor data, specifically angular velocities and linear accelerations. The resulting simulation contains spatiotemporal, kinetic, and kinematic information. Furthermore, the tracking approach avoids integration of the inertial sensor measurements and thus the related integration drift. We previously showed that with this approach, we could estimate joint angles and joint moments similar to those obtained through inverse kinematics and inverse dynamics based on OMC and ground reaction force measurements [20].

However, estimating both kinetics and kinematics from inertial sensor data commonly requires a sensor on each body segment of interest. For example, to estimate leg kinematics and kinetics using optimal control, 7 inertial sensors were used for a sagittal plane estimation [20]. Another setup combined inertial data of 8 sensors to estimate leg kinematics and kinetics, including three dimensional information for the hip and pelvis [21]. A full-body estimation, including the upper body as well, required 17 sensors [12]. When more sensors are placed on the body, the wearer, and thus their motion, will be increasingly affected. Furthermore, too many sensors increase cost, reduce practicality, and increase the chance of errors in IMU placement [22]. Therefore, our aim is to create an IMC system that is as unobtrusive as possible by reducing the number of necessary sensors. Such systems have been developed to provide spatiotemporal (e.g., [1]), sagittal plane kinematic [22–24], three dimensional kinematic [25] or sagittal plane kinetic [26] gait variables. These methods do not provide a comprehensive analysis considering spatiotemporal, kinematic, and kinetics characteristics of gait. On the one hand, neural networks have been investigated to estimate specific quantities of interest using only two IMUs, mounted on the left and right shank [22] or the feet [1, 24] without considering physical correctness. On the other hand, physics-based optimization has been proposed to track the orientation of shank-mounted sensors with a torque-driven model [26] or to track the signals of six IMUs with a human body shape model [25]. To our knowledge, no systematic comparison has been performed to evaluate different sensor configurations for estimating spatiotemporal variables, kinematics, and kinetics during walking and running.

In this work, we performed such a systematic comparison in this paper to evaluate how well spatiotemporal variables, joint kinetics, and joint kinematics can be estimated from sparse sensor setups using an optimal control approach. Previously, an optimal control approach was developed for a full lower-body sensor setup [20]. Since realistic walking simulations of musculoskeletal models can also be created by solving optimal control problems with no data tracking [27], it should be possible to apply the approach developed by [20] to sparse sensor setups as well. Here, we therefore investigated the accuracy of reconstructive simulations created by solving optimal control problems for different sparse sensor setups. We created these different sensor setups by varying the number of IMUs included as well as the body segments on which they were attached. We then created optimal control simulations of walking and running for each sensor setup and investigated the difference between the resulting spatiotemporal variables, gait kinematics, and gait kinetics, and those obtained using OMC and using the full lower-body sensor setup as used by [20].

Methods

We reconstructed walking and running motions of a sagittal-plane musculoskeletal model using raw inertial sensor measurements, i.e., raw gyroscope and accelerometer data, from six different sparse sensor setups and one full lower-body sensor setup (see Fig. 1). Sensors were placed symmetrically for all setups, and each setup included sensors at the feet. We included feet sensors in all setups, since these sensors can be attached to the shoe, and are therefore unobtrusive, while they have also provided reliable information in past studies [1]. For each sensor setup, we created musculoskeletal model simulations by solving optimal control problems that minimized the difference between measured and virtual sensor data. To evaluate the different sensor setups and their respective simulations, we compared the difference between these simulations and an OMC analysis.

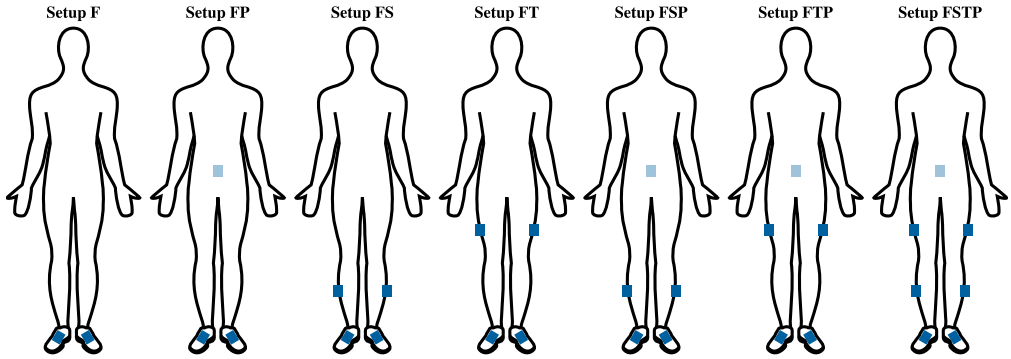

Fig 1. Sensor setups. The blue rectangles indicate the approximate location of the inertial measurement units (IMUs). The sensor setups are abbreviated using the first letter of the segments equipped with a sensor: F-feet, S-shanks, T-thighs, P-pelvis. The setup FSTP corresponds to a full lower-body sensor setup with seven IMUs.

Musculoskeletal Model and Dynamics

We used a sagittal-plane musculoskeletal model to create our gait simulations [20, 28]. The skeleton consisted of seven segments: head-arms-trunk (HAT), two upper legs, two lower legs, and two feet, and had nine kinematic degrees of freedom $\mathbf{q}$: the position and orientation of the trunk, two hip angles, two knee angles, and two ankle angles (Fig. 2).

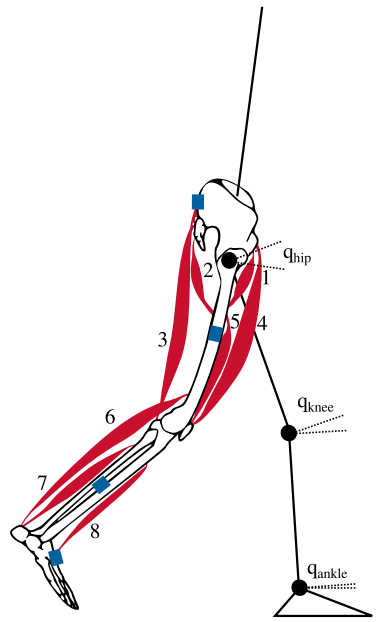

Fig 2. Musculoskeletal model with seven rigid segments and 16 Hill-type-muscles, eight per leg: 1 – iliopsoas, 2 – glutei, 3 – hamstrings, 4 – rectus femoris, 5 – vasti, 6 –gastrocnemius, 7 – soleus, and 8 – tibialis anterior. The blue rectangles indicate the approximate location of the inertial measurement units (IMUs).

We personalized the musculoskeletal model's segment masses, lengths, center of mass locations and moments of inertia based on the study participants' full-body height and weight [29]. The degrees of freedom, together with their first derivative, $\mathbf{v}$, describe the skeleton's state. 16 lower-leg muscles were modeled as three-element Hill-type muscles with states $\mathbf{l_{CE}}$, the length of the contractile element, and $\mathbf{a}$, the muscular activation [30] (Fig. 2). Two contact points at each foot (heel and toe) were defined to model the foot-contact interaction [20]. Each contact point was described by its (x, y) position, and the horizontal (F_x) and vertical (F_y) force. Details about the contact dynamics are further described in [31]. Overall the model's state, $\mathbf{x}$, was described as follows:

$$\mathbf{x} := \begin{bmatrix} \mathbf{q} & \text{nine generalized coordinates} \\ \mathbf{v} & \text{nine generalized velocities} \\ \mathbf{l_{CE}} & \text{16 contractile element lengths} \\ \mathbf{a} & \text{16 muscle activations} \\ [x_1, y_1, F_{x1}, F_{y1}]^T & \text{unknowns 1st contact point} \\ [x_2, y_2, F_{x2}, F_{y2}]^T & \text{unknowns 2nd contact point} \\ [x_3, y_3, F_{x3}, F_{y3}]^T & \text{unknowns 3rd contact point} \\ [x_4, y_4, F_{x4}, F_{y4}]^T & \text{unknowns 4th contact point} \end{bmatrix}. \tag{1}$$

The model was controlled through the 16 muscle excitations, $\mathbf{u}$ [20]. The system dynamics at each time point were fully described by implicit differential equations as a function of $\mathbf{x}$, $\dot{\mathbf{x}}$ and $\mathbf{u}$: $\mathbf{f}(\mathbf{x}, \dot{\mathbf{x}}, \mathbf{u}) = \mathbf{0}$. The system dynamics, $\mathbf{f}()$, were twice differentiable with respect to $\mathbf{x}$, $\dot{\mathbf{x}}$ and $\mathbf{u}$ [20], such that the optimal control problems can be solved using a gradient-based optimization algorithm.

We simulated virtual IMU data using a virtual sensor model that was added to the musculoskeletal model [20]. We placed virtual sensors in their respective position, as measured during the experiment, on the musculoskeletal model, and calculated the virtual sagittal plane accelerometer and gyroscope data from the model state and its

derivative [20].

Optimal Control Problems

We created gait simulations from inertial sensor data by solving optimal control problems. In these optimal control problems, an optimization was solved to find a periodic walking or running cycle that minimized muscular effort, while also tracking the measured inertial sensor data. We constructed the tracking objective to minimize the squared difference between measured accelerations and angular velocities from the IMUs and simulated accelerations and angular velocities from the virtual sensor model. These objective terms yielded the following optimal control problem [20, 30]:

$$\underset{\mathbf{u},v}{\text{minimize}} \quad J(\mathbf{x},\mathbf{u},t) = \frac{W_{eff}}{Tv^2 n_{mus}} \int_{t=0}^{T} \sum_{i=1}^{n_{mus}} u_i^2(t)\mathrm{d}t + \tag{2}$$

$$\frac{1}{T n_{track}} \int_{t=0}^{T} \sum_{j=1}^{n_{track}} \left(\frac{y_{j,track}(t) - \mu_{j,track}(t)}{\sigma_{j,track}(t)} \right)^2 \mathrm{d}t \tag{3}$$

$$\tag{4}$$

$$\text{subject to:} \quad \mathbf{f}(\mathbf{x},\dot{\mathbf{x}},\mathbf{u}) = \mathbf{0} \quad \text{(system dynamics)} \tag{5}$$

$$\mathbf{x}_L \leq \mathbf{x} \leq \mathbf{x}_U \quad \text{(bounds on states)} \tag{6}$$

$$\mathbf{u}_L \leq \mathbf{u} \leq \mathbf{u}_U \quad \text{(bounds on controls)} \tag{7}$$

$$\mathbf{x}(T) = \mathbf{x}(0) + vT\mathbf{x}_{hor} \quad \text{(periodicity)}, \tag{8}$$

where $W_{eff} = 300$ is the weighting of the effort term, T the duration of the gait cycle, which was prescribed, v the velocity, which was optimized, n_{mus} the number of muscles, n_{track} the number of tracked variables, $y_{j,track}$ the virtual variable j, either angular velocity or linear acceleration of one of the sensors of one axis, $\mu_{j,track}$ the mean of the respective experimental data, $\sigma_{j,track}$ its standard deviation, and x_{hor} a vector of states to which a horizontal displacement applies (the horizontal pelvis position and the horizontal contact point positions). We also added a regularization term to aid the optimization process [20].

In the different optimal control problems, we varied the number of tracked sensors between three and seven sensors in seven different setups (see Fig. 1). We used measured data previously recorded with an IMC system, consisting of seven custom-built IMUs (Portabiles HealthCare Technologies GmbH, Erlangen, Germany) placed on the pelvis, legs and feet (Fig. 1, setup FSTP). This dataset contained recordings of 10 healthy male participants (age: 27.1 ± 2.6 years, height: 181.9 ± 5.3 cm, weight: 76.9 ± 8.6 kg) at six different speeds (slow walking: 0.9-1.0 $\mathrm{m\,s^{-1}}$; normal walking: 1.3-1.4 $\mathrm{m\,s^{-1}}$; fast walking: 1.7-1.8 $\mathrm{m\,s^{-1}}$; slow running: 3.1-3.3 $\mathrm{m\,s^{-1}}$; normal running: 3.9-4.1 $\mathrm{m\,s^{-1}}$; fast running: 4.7-4.9 $\mathrm{m\,s^{-1}}$). This dataset was previously used to evaluate inertial sensor data of the full lower-body sensor setup (setup FSTP) [20]. Here, we evaluated six sensor setups with sparser sensor placement (Fig. 1, setup F, FP, FS, FT, FSP, and FTP), and compared those to the full lower-body sensor setup and OMC data.

To solve the optimal control problems, we transcribed them using direct collocation with a backward Euler discretization and $N = 100$ time nodes [20, 30]. We used the same initial guess and the same objective weights as [20]. We solved the resulting large scale nonlinear optimization problems with IPOPT [32].

Data Analysis

We analyzed the convergence of the optimal control problems, followed by a comparison of the spatiotemporal variables, and the kinetic and kinematic variables. First, we

determined the speed as the translation of the right heel divided by the duration of the gait cycle, the stance time as the ratio of the duration of the stance phase [33] and the duration of the gait cycle, and the step length as half the translation of the right heel. To compare spatiotemporal variables, we quantified the similarity of speed, stance time, and step length between the different IMC setups and the OMC setup using the Pearson's correlation coefficient and root mean square deviation (RMSD). For each walking and running speed, we calculated the Pearson's correlation and RMSD between the results calculated with the different inertial sensor setups and the results of the OMC analysis over all participants. Next, we compared kinetic and kinematic trajectories, specifically sagittal joint angles, joint moments, and ground reaction forces of the right leg between the results calculated with the different inertial sensor setups and the results of the OMC analyis using the coefficient of multiple correlation (CMC) [34] and RMSD. We calculated the CMC and the RMSD for each walking or running cycle of each participant individually and then determined the mean (using Fisher's Z-transform for the CMC) over all walking and running cycles and participants. We computed the CMC and RMSD for the entire gait cycle for the joint angles and for the stance phase for the joint moments and ground reaction forces.

Results

We solved 420 simulations, i.e., simulations for seven setups for ten participants at six speeds, on a computer cluster using one Intel Xeon E3-1240 v6 for each simulation. The optimizations required a mean ± standard deviation CPU time of 48 ± 3 min. 418 of the 420 simulations converged, while no optimal solution was found for two simulations. For one participant, the restoration phase failed for setup FP in the slow walking trial, while for another participant, this happened for setup F in the fast walking trial. We removed these two simulations from the analysis.

We found that the correlations and RMSDs of the spatiotemporal variables were similar between all sensor setups, though for speed and step length, a general trend is visible towards higher accuracy with more sensors, and setup F performed worst (see Fig. 3). For speed and step length, setup F generally performed worst for most walking and running conditions, i.e., had the lowest correlations (speed:[1] [−0.35; 0.58]; step length: [0.30; 0.89]) and highest RMSDs (speed: [0.15; 0.55] m/s; step length: [0.08; 0.21] m). When using a sensor on the pelvis in addition to the sensors on the feet (setup FP), speed and step length improved, i.e., the correlations increased (speed: [0.46; 0.80]; step length: [0.66; 0.94]) and the RMSDs decreased (speed: [0.03; 0.36] m/s; step length: [0.02; 0.12] m). The setups without a sensor on the thighs (setups FP, FS, and FSP), resulted in lower RMSDs for speed and step length. However, for running, step length had a similar correlation for all setups, but varied over slow, normal, and fast running. For the stance time, the correlations decreased with an increasing number of sensors for fast walking and running, while the correlations were similar among setups for the slow and normal walking and running speeds. For the setups with sensors only on the lower leg segments (setups F and FS), the stance time RMSD was worst, i.e., up to 27.2 ms higher than the full sensor setup (setup FSTP).

When visualizing the mean of our simulations for each setup with stick figures, we found that the simulations without a pelvis sensor had more forward trunk lean than the full sensor setup (Fig. 4). We also observed that the step length for setup F is larger than the step length of all other setups for walking and running, supporting the larger RMSDs shown in Fig. 3. Furthermore, during walking, a difference in knee flexion angle is visible, where the solutions with thigh sensors have a larger knee flexion angle than

[1] We use the notation [minimum value; maximum value] to show the range of the evaluation criteria.

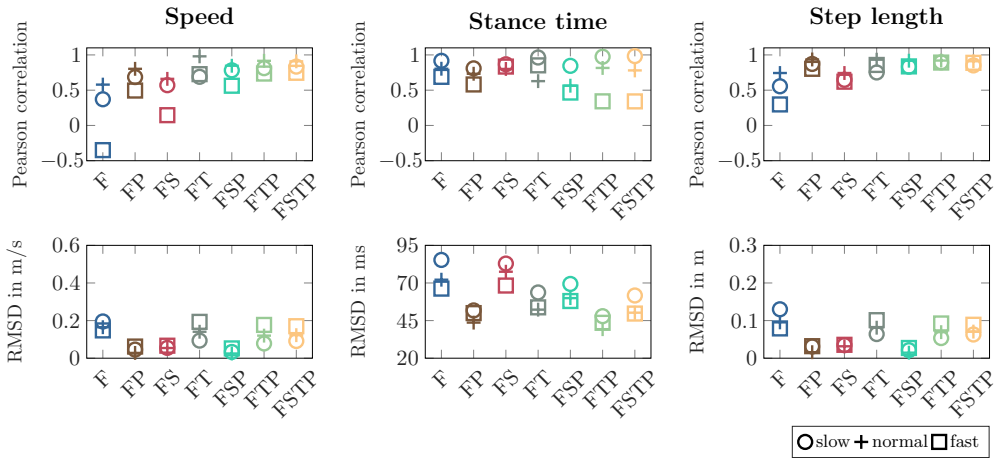

(a) Walking

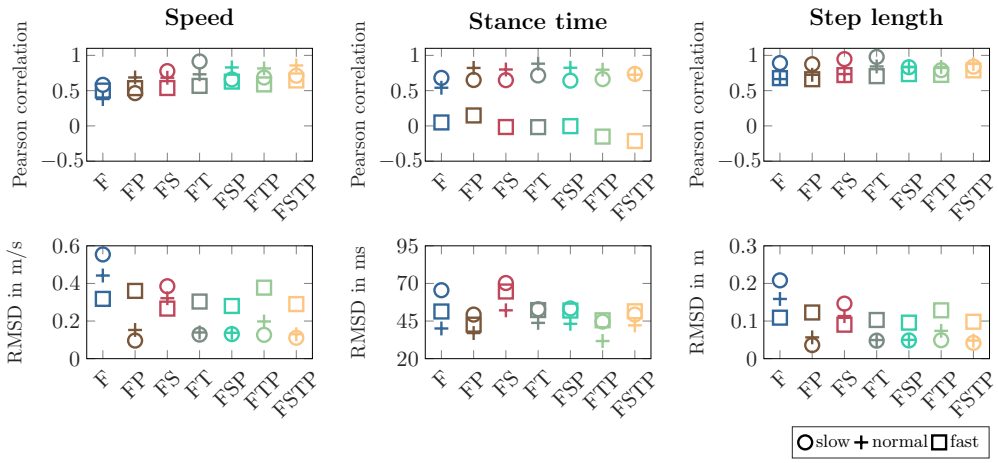

(b) Running

Fig 3. Pearson's correlation and root mean square deviation (RMSD) for speed, stance time, and step length between the different inertial motion capture (IMC) setups and the optical motion capture (OMC) for (a) walking and (b) running.

those without.

Our simulations showed that lower limb kinetics and kinematics generally benefitted from having a sensor at the pelvis, and to a lesser extent from having sensors at the thigh. For setup F, knee flexion was too high during stance for both walking and running, and so was the peak knee extension moment. The peaks in the anterior-posterior and vertical ground reaction force were also too high. Furthermore, the peak ankle dorsiflexion angle was too high as well during running. For setups without thigh sensors (F, FP, FS, and FSP), we also observed for the walking simulations that the joint range of motion of the hip was larger than in the OMC result, and so was the knee extension during late stance, while the forward progression of the ankle dorsiflexion was too fast as well. For these sensor setups, a similar fast progression was observed for the ankle plantarflexion moment, and a similar peak in the knee flexion moment during late stance, while for setup FS the peak hip flexion moment was also too late. For running, the peak hip flexion angle was larger than for the OMC result in the setups without thigh sensors. Furthermore, the anterior-posterior ground reaction force displayed too much braking and push-off for all IMC setups, most prominently for

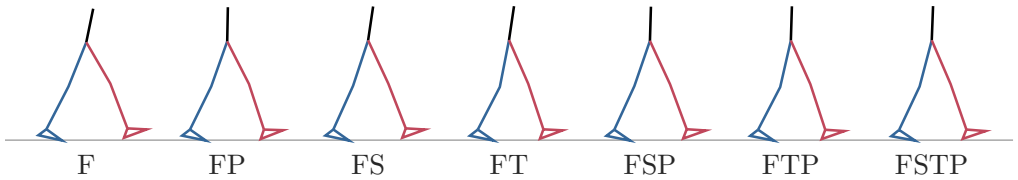

(a) Walking

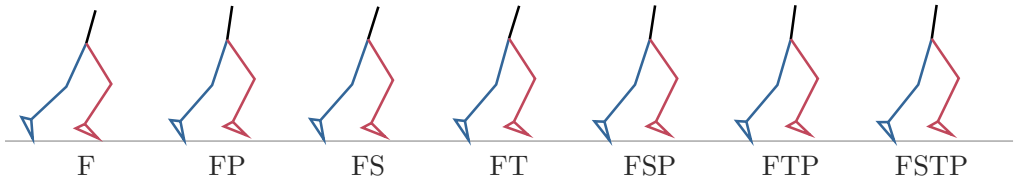

(b) Running

Fig 4. Stick figure representing the mean kinematics at the first time point of the different inertial motion capture (IMC) setups for (a) walking and (b) running, showing that without a pelvis sensor (setups F, FS, and FT), forward trunk lean is too large.

setup F, while the peak vertical ground reaction force was too high for setups F and FS.

We found that how the CMCs changed with the sensor setup varied between the different kinematic and kinetic variables (Fig. 6). The CMCs of the joint angles, ankle joint moment, and ground reaction forces for walking, as well as of the joint angles for running were generally worst for setup F, and there was an improvement in CMC with an increasing number of sensors. For these variables, the mean CMCs decreased considerably from setup FSTP ([0.94; 1.0]) to setup F ([0.88; 0.98]), while they decreased less from setup FSTP to setup FP ([0.92; 0.99]). We could not identify a trend for the CMC of the hip and knee moment during walking and running and the anterior-posterior ground reaction force during running. The CMCs worsened slightly with an increasing number of sensors for the ankle moment and the vertical ground reaction force during running. For example, from setup F to setup FSTP, the mean CMC of the ankle moment and the vertical ground reaction force of running decreased from 0.99 to 0.97 and 0.99 to 0.98, respectively. Furthermore, while the range of CMC values was small for the joint angles, ankle moments, and ground reaction forces, there was a larger variation for the hip and knee joint moment, where some simulations did not correlate with the OMC result at all.

We found similar changes for the RMSD as for the CMC (Fig 7). Similar to the CMC, the RMSD was highest, i.e., worst, for setup F for the joint angles, ankle joint moment, and ground reaction forces during walking, and the hip and knee angle during running, while there is a trend of an improving RMSD with increasing number of sensors. For these variables, the mean RMSDs increased between 46% and 116% from setup FSTP to setup F, while they increased only up to 39% from setup FSTP to setup FP. Only for the ankle angle during running, the RMSDs remained similar, while the CMCs were worst for setup F and improved with an increasing number of sensors. Also similar to the CMC result is that the RMSDs for the ankle moment and vertical ground reaction forces during running were best for setup F and worsened with the increasing number of sensors. For example, from setup F to setup FSTP, the mean RMSD of the ankle moment and the vertical ground reaction force of running increased from 1.9 BW BH % to 4.5 BW BH % and 0.21 BW to 0.49 BW, respectively. Furthermore, we could also not identify a trend for the RMSDs of the hip and knee moment during walking and running and the anterior-posterior ground reaction force during running. The ranges of RMSDs of the hip and knee moments were similar to the range of the

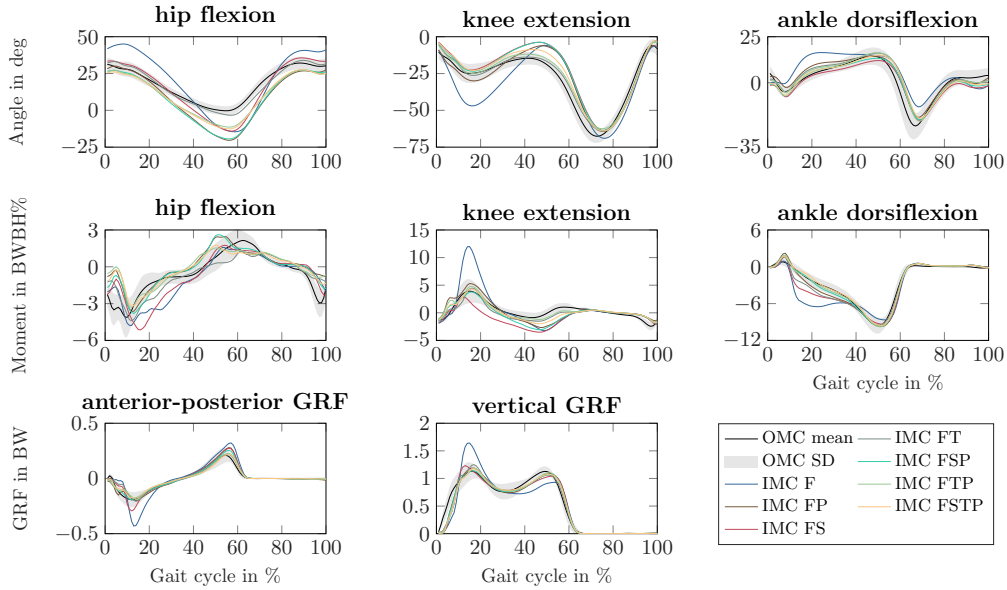

(a) Walking

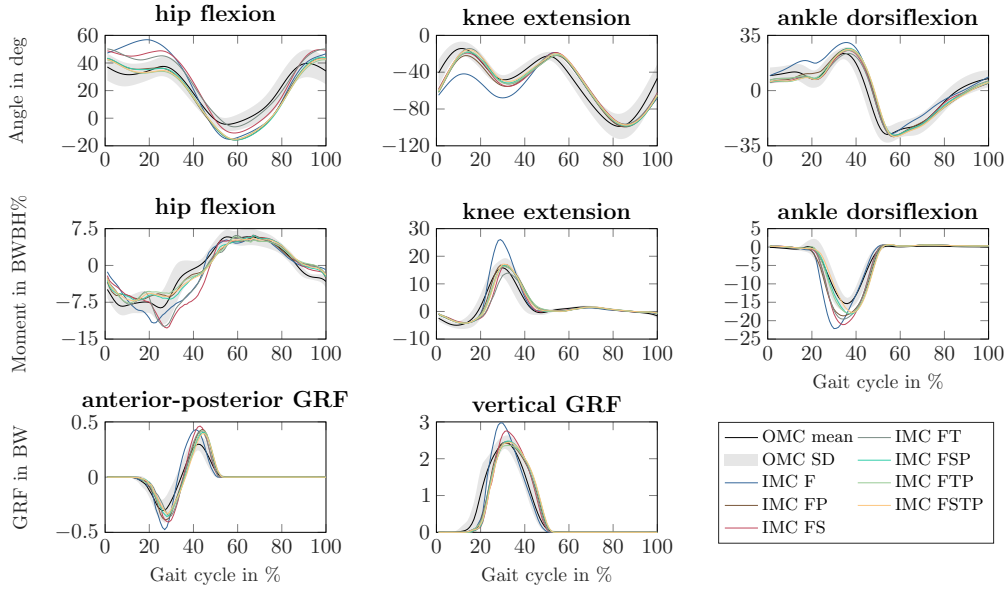

(b) Running

Fig 5. Mean sagittal-plane joint angles, joint moments, and ground reaction forces (GRFs) of the lower limb for (a) walking and (b) running at all speeds, from the different inertial motion capture (IMC) setups (colored lines) and the optical motion capture (OMC) (mean: black line, standard deviation: grey fill). Joint moments were scaled to body-weight body-height percent (BW BH %) and GRFs were scaled to body-weight (BW).

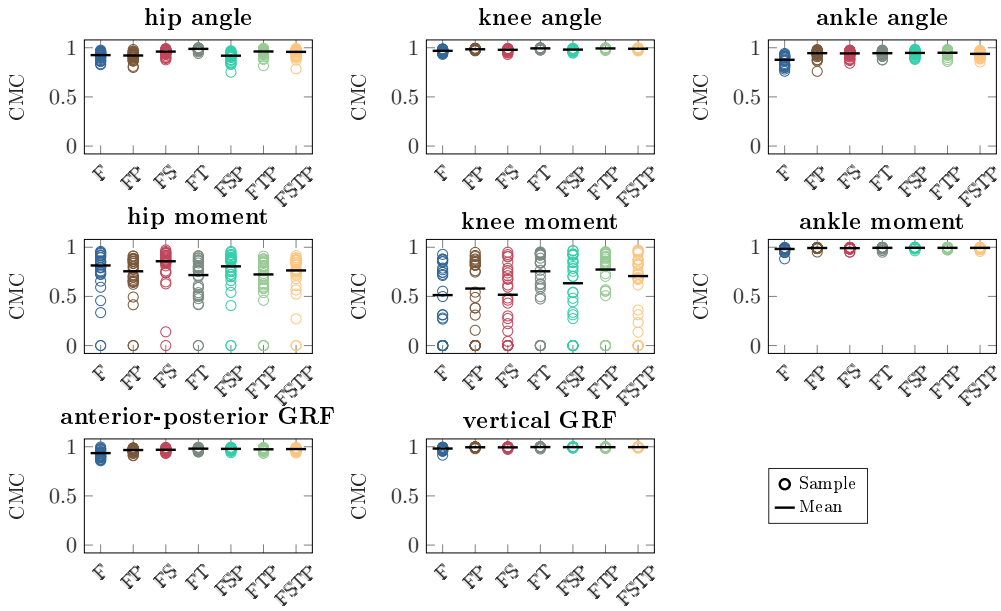

(a) Walking

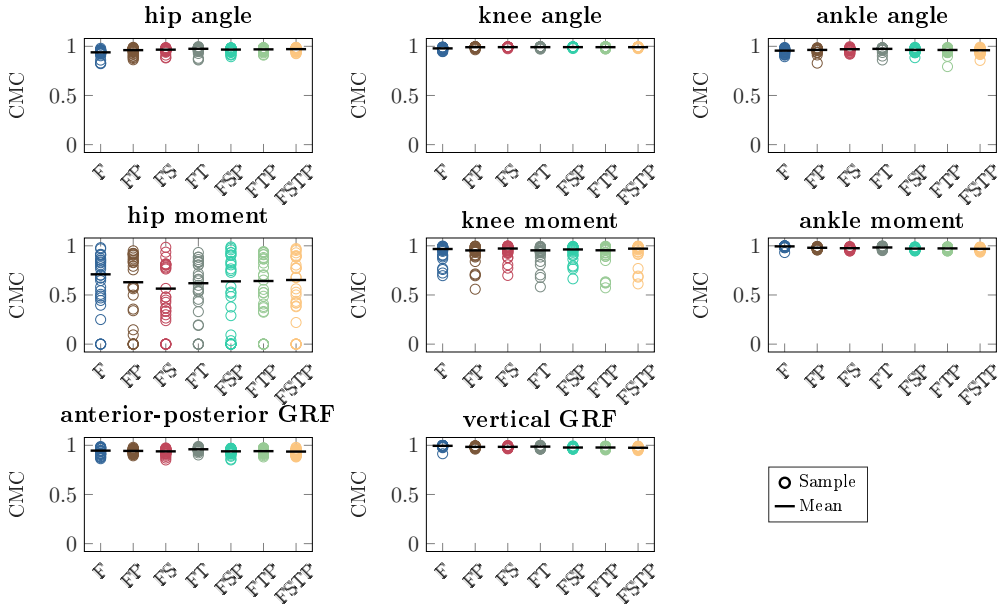

(b) Running

Fig 6. Coefficient of multiple correlation (CMC) for the sagittal-plane joint angles, joint moments, and ground reaction forces (GRFs) between the different inertial motion capture (IMC) setups and optical motion capture (OMC) for (a) walking and (b) running. The circles show the CMC for each walking and running cycle of each participant. The bar shows the mean value over all cycles and participants computed using Fisher's Z-transform.

ankle moment, though still slightly larger, while for the CMCs, the difference in ranges between the hip and knee moment and the ankle moment was larger.

Discussion

We evaluated IMC-based motion analysis using six different sparse sensor setups by comparing their accuracy against OMC-based motion analysis to the accuracy of an IMC-based analysis with a full lower-body sensor setup against the same OMC-based motion analysis. We found that in general it is beneficial to use more than only two sensors at the feet, since RMSD and correlation improved or remained similar for the spatiotemporal variables, and so did the RMSD and CMC for most kinetic and kinematic variables (Fig. 3, Fig. 7, and Fig. 6). For the spatiotemporal, especially for walking, adding sensors to the thighs reduced prediction accuracy (Fig. 3), while adding thigh sensors improved similarity of the kinetic and kinematic patterns (Fig. 5). Surprisingly, increasing the number of sensors reduced accuracy of the vertical ground reaction force and ankle moment during running, while no trend could be identified for the hip and knee moment during both walking and running.

We have shown that it is possible to create sagittal-plane reconstruction of walking and running kinetics and kinematics from sparse sensor setups with high accuracy and small errors, since we were able to create reconstructions with only three sensors (on the feet and the pelvis) that had only a few noticeable differences to those created with a full lower-body sensor setup. These results imply that the improved usability of having only three sensors does not lead to a considerable performance drop of the movement reconstructions. Our results support previous work that showed that, while such movement reconstructions are possible using only foot sensors, results are worse in this approach [20]. In contrast, deep neural networks that directly map foot-worn sensor data to lower-leg kinematics have shown promising results [24]. However, the output of a neural network may be physically incorrect and hard to interpret. One interesting direction for future work would be to combine deep learning and physics-based optimization to obtain physically correct human motion from deep neural networks [35].

We also found that the optimal sensor setup depends on the application variables of interest. For example, predictions of spatiotemporal variables were less accurate when thigh sensors were added, while kinetic and kinematic patterns generally became more accurate by adding these sensors. Another example of this is that during running, accuracy of ground reaction forces and ankle moments are most accurate for setup F.

The kinetics of the reconstruction showed surprising results, specifically the large range in CMC for the hip and knee moment, and the reduction in prediction accuracy during running for the ankle moment and the vertical ground reaction force. The large range in CMC for the hip and knee moment can be explained by the differences between the processing of the OMC and IMC data. The processing of the OMC data included filtering, followed by inverse kinematics and inverse dynamics [29] with a different underlying model. It might be that the low-pass cut-off frequency in our filter was too high, allowing for more high frequency signal to pass than feasible in the optimal control simulation. This would especially affect the CMC but not the RMSD, as we observed in our results. Furthermore, the general differences in processing yield that the kinetics and kinematics of the OMC result cannot be reproduced exactly in an optimal control simulation. This comparison is therefore challenging, since the exact ground truth is unknown, as joint moments and joint angles cannot be measured directly. To remove most differences between the IMC and OMC data, and make the comparison as direct as possible, the optimal control simulations tracking IMC data could be compared against optimal control simulations tracking marker and ground reaction force [36].

Furthermore, the setup of the optimal control problem used for the biomechanical

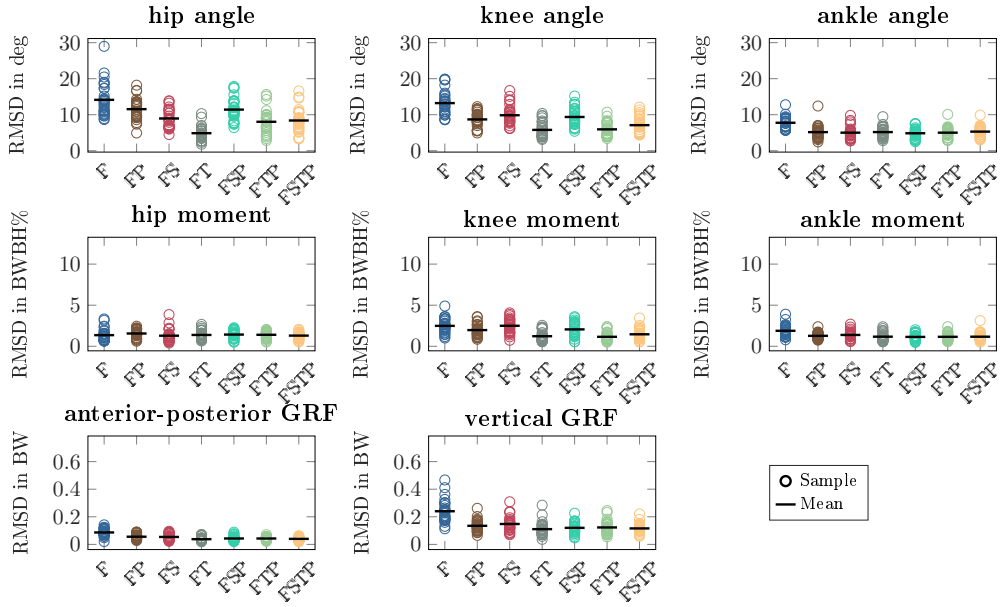

(a) Walking

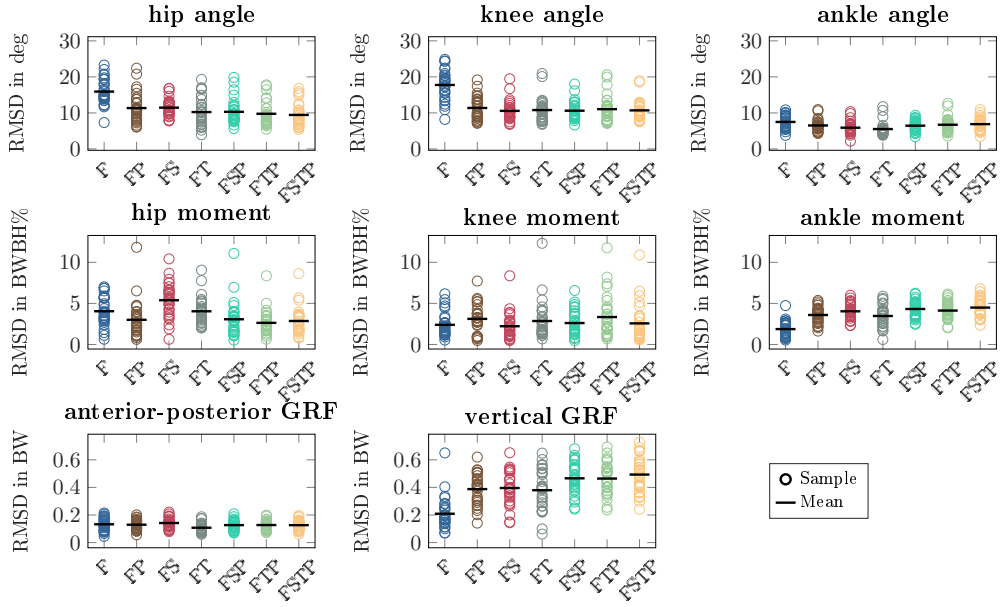

(b) Running

Fig 7. Root mean square deviation (RMSD) for the sagittal-plane joint angles, joint moments, and ground reaction forces (GRFs) between the different inertial motion capture (IMC) setups and optical motion capture (OMC) for (a) walking and (b) running. The circles show the RMSD for each walking and running cycle of each participant. The bar shows the mean value over all cycles and participants. Joint moments were scaled to body-weight body-height percent (BW BH %) and GRFs were scaled to body-weight (BW).

reconstructions could also affect the accuracy of the simulations, and could explain the reduction in accuracy with a higher number of sensors for the ankle moment and vertical ground reaction force. For example, our musculoskeletal model consists of a rigid foot with two penetration-based contact points, one at the heel and one at the toe. These model differences cause different kinetics to be associated with these kinematics for the musculoskeletal model than for the experimental participants, such that the joint moments as recorded by the OMC cannot be achieved. The effect of this foot-ground model on the ankle moment accuracy was already observed for the full lower-body sensor setup [20]. However, it might be possible that with a lower number of sensors, the optimization is solving towards a simulation with more difference in kinematics, but more similarity in the kinetics, while the kinematics match better using more sensors at the cost of reduced accuracy. Another choice in the optimal control setup is the weighting between the effort and tracking objective. We chose our weighting based on [20] and normalized it to the number of sensors to ensure that the objective value was similar for all setups. This weight term could still be tuned individually for each sensor setup, and could even be tuned for each sensor. For example, a larger weight on the pelvis sensor could improve accuracy, especially in a sparse sensor setup, because we found that its inclusion in the sensor setup is important.

Different sensor setups could be investigated to further optimize both usability and accuracy. For example, a sensor setup with three sensors on the shanks and the pelvis could be considered. We chose the setup with sensors on the feet to include as many body segments as possible between the sensors, because no information would be available about the feet when sensors are placed on the shank. Furthermore, it might be possible to increase sparsity by placing sensors asymmetrically on different body segments when symmetric motions are recorded, to avoid double recording of the same signal, e.g., on the left shank and right thigh. Such setups could be further investigated using an observability analysis to investigate the exact working conditions in which kinetics and kinematics can be inferred from simulated inertial measurement data. So far, such an analysis has been performed using recurrent neural networks (RNNs) to estimate the observability of kinematics on simplified mechanical linkages [37]. Nevertheless, in future work such an RNN-based observability analysis might be used to study the observability of both kinematic and kinetic states in sparse IMU setups, for realistic biomechanical kinematic chains, such as we used here.

These results will help those interested in studying motion "in the wild", or outside of the lab environment, since we have shown that using sparse sensor setups will not necessarily reduce accuracy of the resulting simulations. Sparse sensor setups with high accuracy enable capturing of real-life data with reduced burden on patients compared to a full-sensor setup. This real-life data can then support decision-making by providing objective data complementing subjective clinical scores. In particular, sensor-based recordings of movement patterns in different patient cohorts are beneficial to deeply understand intra- and interday variability of motor impairments of chronic diseases. This understanding is of major importance to characterize subgroups of patients or develop personalized approaches in order to evaluate disease progression and therapy response. The real-life data could also help detect changes early in the disease course, which is highly relevant for applying disease-stage-specific therapies. Future studies should evaluate the accuracy, usability as well as the technical and clinical validity of a sparse sensor setup in patients with movement disorders. This would set the basis for robust and valid sensor-based data recordings in real-life with the long-term goal to improve daily care and quality of life of patients using digital technologies.

In conclusion, our work shows that sagittal-plane reconstruction of walking and running kinetics and kinematics from sparse sensor setups are feasible. The reconstruction accuracy generally decreases with a smaller number of sensors, though

not for all calculated variables. Furthermore, the reduction in accuracy will be acceptable for certain applications, such as motion recordings at home, given the improved usability of sparse sensor setups. This study serves as a first step towards validating sparse inertial sensor sets for monitoring movements "in the wild". Future validation studies should ensure that the processing between the IMC and the ground truth measurement is as similar as possible, to avoid including processing differences in the results. This way, validity and usability of sparse sensor setups can be further evaluated for specific applications in order to allow the use of gait analysis in a wide spectrum of clinical and sports applications.

Funding

This project was supported by the German Research Foundation (DFG, Deutsche Forschungsgemeinschaft) under Grant SFB 1483–Project-ID 442419336 "EmpkinS" (ED, MN, BME, ADK), and Project-ID 438496663 "Mobility_APP" (HG, BME). ADK was also supported by faculty endowment from adidas AG. Furthermore, the HPC resources were provided by the Erlangen National High Performance Computing Center (NHR@FAU) of the Friedrich-Alexander-Universität Erlangen-Nürnberg (FAU). HG and BE are supported by the Mobilise-D project that has received funding from the Innovative Medicines Initiative 2 Joint Undertaking under grant agreement 820820, which receives support from the European Union's Horizon 2020 research and innovation program and the European Federation of Pharmaceutical Industries and Associations. HG was further supported by the Fraunhofer Internal Programs under grant Attract 044-602140 and 044-602150.

References

1. Jakob V, Küderle A, Kluge F, Klucken J, Eskofier BM, Winkler J, et al. Validation of a sensor-based gait analysis system with a gold-standard motion capture system in patients with Parkinson's disease. Sensors. 2021;21(22):7680.

2. Ferris AE, Aldridge JM, Rábago CA, Wilken JM. Evaluation of a powered ankle-foot prosthetic system during walking. Archives of physical medicine and rehabilitation. 2012;93(11):1911–1918.

3. Mohr M, Federolf P, Heinrich D, Nitschke M, Raschner C, Scharbert J, et al. An 8-week injury prevention exercise program combined with change-of-direction technique training reduces change-of-direction knee joint loading without compromising performance; 2023.

4. Liu T, Inoue Y, Shibata K. Development of a wearable sensor system for quantitative gait analysis. Measurement. 2009;42(7):978–988. doi:10.1016/j.measurement.2009.02.002.

5. Weygers I, Kok M, Konings M, Hallez H, de Vroey H, Claeys K. Inertial Sensor-Based Lower Limb Joint Kinematics: A Methodological Systematic Review. Sensors (Basel, Switzerland). 2020;20(3). doi:10.3390/s20030673.

6. Uhlrich SD, Falisse A, Kidziński Ł, Muccini J, Ko M, Chaudhari AS, et al. OpenCap: 3D human movement dynamics from smartphone videos. bioRxiv. 2022; p. 2022–07.

7. Nakano N, Sakura T, Ueda K, Omura L, Kimura A, Iino Y, et al. Evaluation of 3D markerless motion capture accuracy using OpenPose with multiple video cameras. Frontiers in sports and active living. 2020;2:50.

8. Zhang JT, Novak AC, Brouwer B, Li Q. Concurrent validation of Xsens MVN measurement of lower limb joint angular kinematics. Physiological measurement. 2013;34(8):N63–9. doi:10.1088/0967-3334/34/8/N63.

9. Fleron MK, Ubbesen NCH, Battistella F, Dejtiar DL, Oliveira AS. Accuracy between optical and inertial motion capture systems for assessing trunk speed during preferred gait and transition periods. Sports biomechanics. 2019;18(4):366–377. doi:10.1080/14763141.2017.1409259.

10. Kobsar D, Charlton JM, Tse CT, Esculier JF, Graffos A, Krowchuk NM, et al. Validity and reliability of wearable inertial sensors in healthy adult walking: A systematic review and meta-analysis. Journal of neuroengineering and rehabilitation. 2020;17:1–21.

11. Ancillao A, Tedesco S, Barton J, O'Flynn B. Indirect measurement of ground reaction forces and moments by means of wearable inertial sensors: A systematic review. Sensors. 2018;18(8):2564.

12. Karatsidis A, Jung M, Schepers HM, Bellusci G, de Zee M, Veltink PH, et al. Musculoskeletal model-based inverse dynamic analysis under ambulatory conditions using inertial motion capture. Medical engineering & physics. 2019;65:68–77.

13. Sabatini AM, Ligorio G, Mannini A. Fourier-based integration of quasi-periodic gait accelerations for drift-free displacement estimation using inertial sensors. Biomedical engineering online. 2015;14(1):1–18.

14. Mundt M, Thomsen W, Witter T, Koeppe A, David S, Bamer F, et al. Prediction of lower limb joint angles and moments during gait using artificial neural networks. Medical & biological engineering & computing. 2020;58:211–225.

15. Yi X, Zhou Y, Xu F. TransPose. ACM Transactions on Graphics. 2021;40(4):1–13. doi:10.1145/3450626.3459786.

16. Conte Alcaraz J, Moghaddamnia S, Peissig J. Efficiency of deep neural networks for joint angle modeling in digital gait assessment. EURASIP Journal on Advances in Signal Processing. 2021;2021(1):1–20.

17. Mundt M, Johnson WR, Potthast W, Markert B, Mian A, Alderson J. A comparison of three neural network approaches for estimating joint angles and moments from inertial measurement units. Sensors. 2021;21(13):4535.

18. Dorschky E, Nitschke M, Martindale CF, Van den Bogert AJ, Koelewijn AD, Eskofier BM. CNN-Based Estimation of Sagittal Plane Walking and Running Biomechanics From Measured and Simulated Inertial Sensor Data. Frontiers in bioengineering and biotechnology. 2020;8:604. doi:10.3389/fbioe.2020.00604.

19. Rapp E, Shin S, Thomsen W, Ferber R, Halilaj E. Estimation of kinematics from inertial measurement units using a combined deep learning and optimization framework. Journal of Biomechanics. 2021;116:110229.

20. Dorschky E, Nitschke M, Seifer AK, Van den Bogert AJ, Eskofier BM. Estimation of gait kinematics and kinetics from inertial sensor data using optimal control of musculoskeletal models. Journal of biomechanics. 2019;95:109278. doi:10.1016/j.jbiomech.2019.07.022.

21. Al Borno M, O'Day J, Ibarra V, Dunne J, Seth A, Habib A, et al. OpenSense: An open-source toolbox for inertial-measurement-unit-based measurement of lower extremity kinematics over long durations. Journal of NeuroEngineering and Rehabilitation. 2022;19(1):1–11.

22. Gholami M, Napier C, Menon C. Estimating lower extremity running gait kinematics with a single accelerometer: A deep learning approach. Sensors. 2020;20(10):2939.

23. Li T, Wang L, Li Q, Liu T. Lower-Body Walking Motion Estimation Using Only Two Shank-Mounted Inertial Measurement Units (IMUs). In: 2020 IEEE/ASME International Conference on Advanced Intelligent Mechatronics (AIM). IEEE; 2020. p. 1143–1148.

24. Hossain MSB, Dranetz J, Choi H, Guo Z. Deepbbwae-net: A cnn-rnn based deep superlearner for estimating lower extremity sagittal plane joint kinematics using shoe-mounted imu sensors in daily living. IEEE Journal of Biomedical and Health Informatics. 2022;26(8):3906–3917.

25. Von Marcard T, Rosenhahn B, Black MJ, Pons-Moll G. Sparse inertial poser: Automatic 3d human pose estimation from sparse imus. In: Computer graphics forum. vol. 36. Wiley Online Library; 2017. p. 349–360.

26. Li T, Wang L, Yi J, Li Q, Liu T. Reconstructing walking dynamics from two shank-mounted inertial measurement units. IEEE/ASME Transactions on Mechatronics. 2021;26(6):3040–3050.

27. Falisse A, Serrancolí G, Dembia CL, Gillis J, Jonkers I, De Groote F. Rapid predictive simulations with complex musculoskeletal models suggest that diverse healthy and pathological human gaits can emerge from similar control strategies. Journal of The Royal Society Interface. 2019;16(157):20190402.

28. Van den Bogert AJ, Hupperets M, Schlarb H, Krabbe B. Predictive musculoskeletal simulation using optimal control: Effects of added limb mass on energy cost and kinematics of walking and running. Proceedings of the Institution of Mechanical Engineers, Part P: Journal of Sports Engineering and Technology. 2012;226(2):123–133. doi:10.1177/1754337112440644.

29. Winter DA. Biomechanics and motor control of human movement. 4th ed. Hoboken, N.J: Wiley; 2009. Available from: `http://dx.doi.org/10.1002/9780470549148`.

30. Van den Bogert AJ, Blana D, Heinrich D. Implicit methods for efficient musculoskeletal simulation and optimal control. Procedia IUTAM. 2011;2(2011):297–316. doi:10.1016/j.piutam.2011.04.027.

31. Todorov E. Implicit nonlinear complementarity: A new approach to contact dynamics. In: 2010 IEEE International Conference on Robotics and Automation. IEEE; 2010. p. 2322–2329.

32. Wächter A, Biegler LT. On the implementation of an interior-point filter line-search algorithm for large-scale nonlinear programming. Mathematical Programming. 2006;106(1):25–57. doi:10.1007/s10107-004-0559-y.

33. Maiwald C, Sterzing T, Mayer Ta, Milani TL. Detecting foot-to-ground contact from kinematic data in running. Footwear Science. 2009;1(2):111–118.

34. Ferrari A, Cutti AG, Cappello A. A new formulation of the coefficient of multiple correlation to assess the similarity of waveforms measured synchronously by different motion analysis protocols. Gait & posture. 2010;31(4):540–542. doi:10.1016/j.gaitpost.2010.02.009.

35. Yi X, Zhou Y, Habermann M, Shimada S, Golyanik V, Theobalt C, et al. Physical inertial poser (pip): Physics-aware real-time human motion tracking from sparse inertial sensors. In: Proceedings of the IEEE/CVF Conference on Computer Vision and Pattern Recognition; 2022. p. 13167–13178.

36. Nitschke M, Marzilger R, Leyendecker S, Eskofier BM, Koelewijn AD. Change the direction: 3D optimal control simulation by directly tracking marker and ground reaction force data. PeerJ. 2023;11:e14852.

37. Bachhuber S, Weber D, Weygers I, Seel T. RNN-based Observability Analysis for Magnetometer-Free Sparse Inertial Motion Tracking. In: 2022 25th International Conference on Information Fusion (FUSION). IEEE; 2022. p. 1–8.